RSC Advances

PAPER

View Article Online
View Journal | View Issue

Cite this: *RSC Adv.*, 2020, **10**, 15299

Phosphate-sensing with (di-(2-picolyl)amino) quinazolines based on a fluorescence on–off system†

Kazusa Aoki, Ryuji Osako, Jiahui Deng, Takashi Hayashita, Takeshi Hashimoto and Yumiko Suzuki *

Received 15th February 2020
Accepted 8th April 2020

DOI: 10.1039/d0ra01455a

rsc.li/rsc-advances

Detection and visualization of phosphates such as ATP in living organisms can facilitate the elucidation of various biological events. Although substantial efforts had been made in this area, present methods have disadvantages such as the need for specialized equipment and poor sensitivities. To address these limitations, novel fluorescent probes, (di-(2-picolyl)amino)quinazolines, were developed for application in ATP detection. They selectively recognized copper ions by fluorescence quenching, and their copper complexes displayed fluorescence enhancement in the presence of phosphoric acid derivatives. This fluorescence on–off system enabled highly sensitive fluorescence detection of ATP when combined with a phenyl boronic acid-modified γ-cyclodextrin through a plausible multipoint recognition system.

Introduction

Phosphates typified by adenosine 5′-triphosphate (ATP) are essential for life and are involved in various biochemical pathways. Therefore, real-time monitoring, visualization, or quantification of phosphate levels, can potentially aid in the elucidation of various biological events and disease mechanisms. The reported approaches for the detection of ATP require specialized and/or costly equipment such as HPLC,[1] NMR,[2] or micro-fluidic chips.[3] To address these limitations, various fluorescent probes such as low molecular weight,[4–6] polymer,[7,8] and supramolecular sensors[9] that enable simpler and efficient detection have been developed. However, these existing strategies have disadvantages such as the necessity for expensive supported metals or proteins, and also suffer from poor sensitivities and selectivities. To further address these challenges, we conducted a study for the development of novel strategies for fluorescence detection of phosphates using a combination of quinazoline fluorophores possessing di-2-(picolyl)amine (dpa) and cyclodextrins (CyDs).

Dpa can complex with various metals, and the dpa-bound fluorophores display diverse fluorescence responses depending on the identity of the complexed metal species.[10] Furthermore, the interaction between dpa–metal complexes and ATP weakens the dpa–metal coordination, which results in changes in the fluorescence of the molecule, which is critical for our design. In fact, dpa–metal complexes are well-known for their recognition of phosphoric acid derivatives, including ATP.[11–16]

CyDs are well-known water-soluble host molecules comprising nano-sized hydrophobic cavities that enable them to incorporate various organic compounds in aqueous solutions.[17] In addition, the structural modifications of CyDs are straightforward, which allow the incorporation of a variety of functionalities for modulating their properties.[18,19] These beneficial properties of CyDs have attracted significant

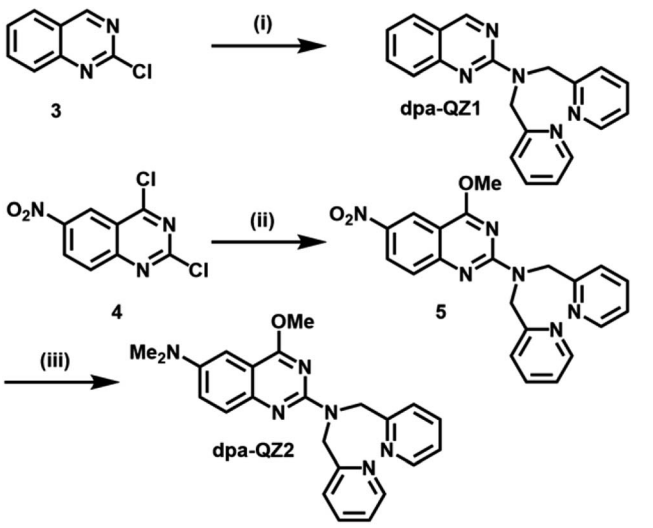

Scheme 1 Synthesis of fluorescent quinazolines **dpa-QZ1** and **dpa-QZ2**. (i) dpa, TEA, THF, reflux, 1 week, 70%. (ii) NaOMe, MeOH, 0 °C, 23 h; 20 °C, 3 h; dpa, reflux 4 h, 68%. (iii) H_2, Pd/C (10 mol%), MeOH, r.t., 2 h; HCOOH, HCHO, reflux, 2 h, 29%. dpa = di-(2-picolyl)amine, TEA = trimethylamine.

Department of Materials and Life Sciences, Faculty of Science and Technology, Sophia University, Kioi-cho 7-1, Chiyoda-ku, Tokyo 102-8554, Japan. E-mail: yumiko_suzuki@sophia.ac.jp

† Electronic supplementary information (ESI) available. See DOI: 10.1039/d0ra01455a

attention for use in various avenues of science and technology, such as in molecular recognition systems,[20,21] supramolecular chemistry,[22,23] and drug delivery systems[24] based on their host–guest interactions. We anticipated that the combination of CyDs and quinazoline fluorophores, recently discovered by our group,[25] could potentially be employed for the development of a highly sensitive phosphate recognition system. We report herein, a novel recognition system for phosphate detection that is based on the (di-(2-picolyl)amino)quinazoline and phenylboronic acid-modified γ-cyclodextrin platforms.

The starting point for this study was the design and synthesis of the quinazoline derivatives **dpa-QZ1** and **dpa-QZ2**, bearing a di-(2-picolyl)amine (dpa) moiety at position 2 of the quinazoline framework as probes for phosphate recognition (Scheme 1).

Experimental

Materials and instrument

Chemicals were supplied by WAKO Pure Chemical Industries, Ltd., Kanto Chemical Co. INC, Tokyo Chemical Industry Co., Ltd., or Sigma-Aldrich, and were used without purification. Column chromatography was performed on Merck Silica Gel 60 or Merck aluminium oxide using chloroform, ethyl acetate and *n*-hexane as eluents. TLC experiments were carried out on Merck Silica Gel 60 F_{254} plates for Merck Silica Gel 60 and on Merck aluminium oxide 60 F_{254} plates for Merck aluminium oxide. Structural identification of the synthesized compounds was confirmed by ^{1}H-NMR, ^{13}C-NMR, HRMS spectroscopy, and elemental analysis. The ^{1}H or ^{13}C nuclear magnetic resonance (NMR) spectra were recorded on a JEOL JNM-ECA500 NMR spectrometer (500 MHz) using TMS and $CDCl_3$ or DMSO-d_6 as internal standards. The ^{1}H-NMR and ^{13}C-NMR spectral data are reported as follows: chemical shift (ppm), integration, multiplicity (s. singlet; d, doublet; t, triplet; q, quartet, m, multiplet), coupling constants (*J*) in Hz. Mass spectra were recorded using a TOF (ESI) analyzer or a magnetic sector (EI and FAB) analyzer. Elemental analysis was conducted with a PerkinElmer PE2400 II apparatus. Melting points were measured using a ATM-02, AS ONE. UV-Vis absorption spectra in solution were recorded at room temperature with a Hitachi U-3900. Fluorescence spectra in solution were recorded at room temperature with a Hitachi F-7000. A quart cuvette with a 1 cm path length was used. Water was doubly distilled and deionized with a Mill-Q water system (WG222, Yamato Sci. Co. Ltd. and Autopure WR-600G, Millipore).

Preparation of fluorescent quinazolines

Synthesis of dpa-QZ1. Under an argon atmosphere, trimethylamine (0.51 mL, 3.65 mmol) and di-(2-picolyl)amine (0.82 mL, 4.56 mmol) were added to a solution of 2-chloroquinazoline[26] (500 mg, 3.04 mmol) in dehydrated THF(20 mL), and the mixture was heated under reflux for 1 week. After cooling, the product was extracted with CH_2Cl_2. The organic layer was washed with brine, and dried over Na_2SO_4. It was then filtered, and concentrated under reduce pressure. The residue was purified by alumina column chromatography (2 : 1 *n*-hexane/ethyl acetate, then 1 : 2) to obtain the desired product (698 mg, 2.13 mmol, 70%) as a yellow solid.

$R_f = 0.33$ (2 : 1 *n*-hexane/ethyl acetate, Al_2O_3 plate).

Mp 118–120 °C.

Yellow needles, recrystallized from dichloromethane/hexane.

^{1}H-NMR ($CDCl_3$, 500 MHz): δ: 9.04 (1H, s), 8.54 (2H, m), 7.66 (2H, t, $J = 9.2$ Hz), 7.56–7.59 (3H, m), 7.30 (2H, s), 7.23 (1H, t, $J = 6.5$ Hz), 7.14 (2H, t, $J = 6.5$ Hz), 5.23 (4H, s).

^{13}C-NMR ($CDCl_3$, 500 MHz): δ: 161.8, 159.5, 158.7, 152.4, 149.4, 136.5, 134.0, 127.3, 126.0, 122.6, 121.9, 121.4, 121.3, 119.9, 52.6.

HRMS (FAB) *m*/*z* calcd for $C_{20}H_{17}N_5$ $(M - H)^-$: 328.1562, found: 328.1551.

Anal. calcd for $C_{20}H_{17}N_5$: C, 73.37%; H, 5.23%; N, 21.39%, found: C, 73.46%; H, 5.26%; N, 21.35%.

Synthesis of compound 4-methoxy-6-nitro-2-di-(2-picolyl) aminoquinazoline (5). Under an argon atmosphere, sodium methoxide (0.50 g, 9.33 mmol) was added to a solution of 2,4-dichloro-6-nitroquinazoline[27] (1.51 g, 6.18 mmol) in dehydrated MeOH (130 mL), and the mixture stirred at 0 °C for 23 h and then 20 °C for 3 h. Then, di-(2-picolyl)amine (1.66 mL, 9.25 mmol) was added to the reaction mixture, which was subsequently heated under reflux with stirring for 4 h. After cooling, the product was extracted with dichloromethane. The organic layer was washed with brine, and dried over Na_2SO_4. And then it was filtered, and concentrated under reduced pressure. The residue was purified by alumina column chromatography (1 : 1 *n*-hexane/ethyl acetate) to obtain the desired product (1.68 g, 68%) as a yellow solid.

$R_f = 0.67$ (1 : 1 *n*-hexane/ethyl acetate, Al_2O_3 plate).

Mp 149–150 °C.

Yellow needles, recrystallized from dichloromethane/hexane.

^{1}H-NMR (500 MHz, $CDCl_3$) δ: 8.84 (1H, d, $J = 2.3$ Hz), 8.56 (2H, s), 8.34 (1H, dd, $J = 9.2$, 2.3 Hz), 7.60–7.65 (2H, m), 7.50 (1H, d, $J = 9.2$ Hz), 7.40 (1H, d, $J = 8.0$ Hz), 7.16–7.23 (3H, m), 5.27 (2H, s), 5.16 (2H, s), 3.97 (3H, s).

^{13}C-NMR (126 MHz, $CDCl_3$) δ: 168.2, 160.5, 158.2, 157.7, 157.0, 149.4, 141.3, 136.6, 127.5, 126.1, 122.2, 122.1, 121.5, 120.9, 110.4, 54.4, 53.1, 52.9.

HRMS (FAB) *m*/*z* calcd for $C_{21}H_{19}N_6O_3$ $(M + H)^+$: 403.1519, found: 403.1533.

Synthesis of dpa-QZ2. Palladium 10% on carbon (0.14 g, 0.13 mmol) was added to a solution of **5** (500 mg, 1.26 mmol) in MeOH (30 mL). Under a hydrogen atmosphere, the mixture was stirred at room temperature for 2 h. The mixture was filtered through Celite® and concentrated under reduced pressure. The resulting residue—crude 6-amino substituted quinazoline—was dissolved in formic acid (25 mL), and then 37% formaldehyde (0.30 mL, 3.77 mmol) solution was added. The mixture was heated under reflux with stirring for 2 h, cooled to room temperature, and neutralized with aqueous sodium hydroxide. The product was extracted with dichloromethane. The combined organic layer was washed with brine, and dried over Na_2SO_4. After the filtration, the organic layer was concentrated under reduced pressure. The residue was purified by alumina column chromatography (1 : 1 *n*-hexane/ethyl acetate) to obtain the desired product (145 mg, 29%) as a yellow solid.

R_f = 0.35 (1 : 1 *n*-hexane/ethyl acetate, Al_2O_3 plate).

Mp 136–137 °C.

Yellow prisms, recrystallized from dichloromethane/hexane.

^{1}H-NMR (500 MHz, $CDCl_3$) δ: 8.53 (2H, d, J = 4.5 Hz), 7.57 (2H, td, J = 7.2, 1.5 Hz), 7.47 (1H, d, J = 9.2 Hz), 7.31 (3H, dd, J = 9.2, 2.9 Hz), 7.12 (2H, m), 7.06 (1H, d, J = 2.9 Hz), 5.16 (4H, s), 3.88 (3H, s), 2.97 (6H, s).

^{13}C-NMR (126 MHz, $CDCl_3$) δ: 166.5, 159.5, 156.8, 149.1, 146.8, 146.3, 136.4, 126.0, 123.3, 121.7, 121.3, 112.0, 103.1, 53.6, 52.8, 41.4.

HRMS (FAB) m/z calcd for $C_{23}H_{24}N_6O$ $(M)^+$: 400.2012, found: 400.2017.

Anal. calcd for $C_{23}H_{24}N_6O$: C, 68.98%; H, 6.04%; N, 20.99%, found: C, 68.97%; H, 5.79%; N, 20.87%.

Synthesis of FPB-γ-CyD. 4-Carboxy-3-fluorophenylboronic acid (44 mg, 0.24 mmol), *N*,*N*′-dicyclohexylcarbodiimide (DCC, 62 mg, 0.3 mmol), and 1-hydroxybenzotriazole ($HOBt\cdot H_2O$, 46 mg, 0.3 mmol) were dissolved in 5 mL of DMF and stirred in an ice bath for 30 min. To this solution, a solution of 259 mg (0.2 mmol) of 3-NH_2-γ-CyD dissolved in 5 mL of DMF was added, and the mixture was stirred in an ice bath for 30 min and at room temperature for 20 h. The solution concentrated by distillation under reduced pressure was stored in a refrigerator for 24 h to remove a reaction by-product. The precipitated by-product was removed by cotton filtration, and the filtrate was poured into 800 mL of acetone while stirring, and the crude product was purified by reprecipitation. The product precipitated in acetone was subjected to suction filtration using a membrane filter (TYPE: JHWP), and the obtained white solid was dissolved in deionized water and lyophilized under reduced pressure to obtain a white powder (188 mg, 65% yield).

^{1}H-NMR (300 MHz, D_2O) δ: 7.8 (t, 1H), 7.62 (d, 1H), 7.5 (d, 1H), 5.2–5.0 (m, 8H), 4.05–3.45 (m, 48H).

Anal. calcd for $BC_{55}H_{85}FNO_{42}\cdot 5.0H_2O$: C, 40.23%; H, 6.44%; N, 0.85%, found: C, 40.20%; H, 6.46%; N, 1.01%.

Synthesis of FPB-β-CyD. **FPB-β-CyD** was synthesized by the similar procedure as shown in the synthesis of **FPB-γ-CyD**. White powder (178 mg, 69% yield).

^{1}H-NMR (300 MHz, D_2O) δ: 8.2–7.2 (m, 3H), 5.25–4.9 (m, 3H), 4.4–3.2 (m, 42H).

Anal. calcd for $BC_{49}H_{75}F\ NO_{37}\cdot 6.5H_2O$: C, 41.53%; H, 6.26%; N, 0.99%, found: C, 41.48%; H, 6.06%; N, 1.01%.

Preparation of solutions for measurements

pH profile. The solutions were prepared in 50 cm^3 volumetric flasks. The pH was adjusted to 2.0 with HCl aqueous solution before the titration with NaOH aqueous solution. In order to avoid remarkable pH jumps, HEPES/NaOH buffer was added, and the ionic strengths were maintained constant with $NaNO_3$ aqueous solution. All the solutions were prepared with 1% DMSO – 99% water (v/v), the concentration of each **dpa-QZ** derivative was 1.0 × 10^{-5} M, HEPES/NaOH buffer was 5.0 × 10^{-3} M and $NaNO_3$ aqueous solution was 0.10 M.

Metal ion recognition. UV-Vis and fluorescence spectra were measured in the presence of 2.0 equivalent of each metal ion: Cu^{2+}, Ni^{2+}, Co^{2+}, Zn^{2+}, Cd^{2+}, and Pb^{2+}. The solutions were prepared with 1% DMSO – 99% water (v/v) in 5 cm^3 volumetric flasks. The concentration of each **dpa-QZ** derivative was 1.0 × 10^{-5} M. The pH of final solutions was adjusted to 7.4 with 5.0 × 10^{-3} M HEPES/NaOH buffer. The ionic strengths were maintained constant by adding 0.10 M $NaNO_3$ aqueous solution.

Phosphoric acid recognition. UV-Vis and fluorescence spectra were measured in the presence of 100 equivalents of each phosphate: monophosphate (Pi), pyrophosphate (PPi), triphosphate (Tri), adenosine monophosphate (AMP), adenosine diphosphate (ADP), and adenosine triphosphate (ATP). The solutions were prepared with 100% water in 5 cm^3 volumetric flasks. The pH of each undiluted solution of phosphate anion was adjusted to 7 with NaOH aqueous solution. The concentration of each **dpa-QZ** derivative was 1.0 × 10^{-5} M. The pH of final measuring solutions was adjusted to 7.4 with 5.0 × 10^{-3} M HEPES/NaOH buffer.

NOESY measurement. The solutions were prepared with d_6-DMSO. The final concentration of **dpa-QZ2** was 8.0 × 10^{-3} M and that of β-CyD was 1.6 × 10^{-2} M.

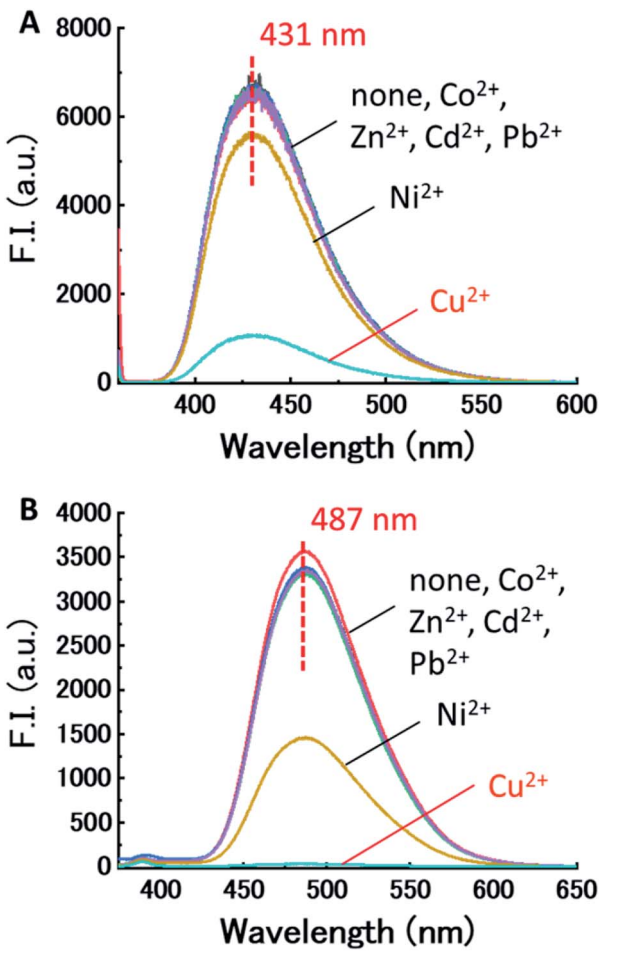

Fig. 1 (A) Fluorescence spectra of (A) **dpa-QZ1** and (B) **dpa-QZ2** with various metals in 1% DMSO – 99% water (v/v), pH 7.4 adjusted using HEPES/NaOH buffer, at 25 °C (λ_{ex}^{1} = 355 nm, $\lambda_{ex}^{dpa\text{-}QZ2}$ = 345 nm). [probe] = 10 μM, [metal$(NO_3)_2$] = 20 μM, [$NaNO_3$] = 0.10 M, [HEPES buffer] = 5.0 mM.

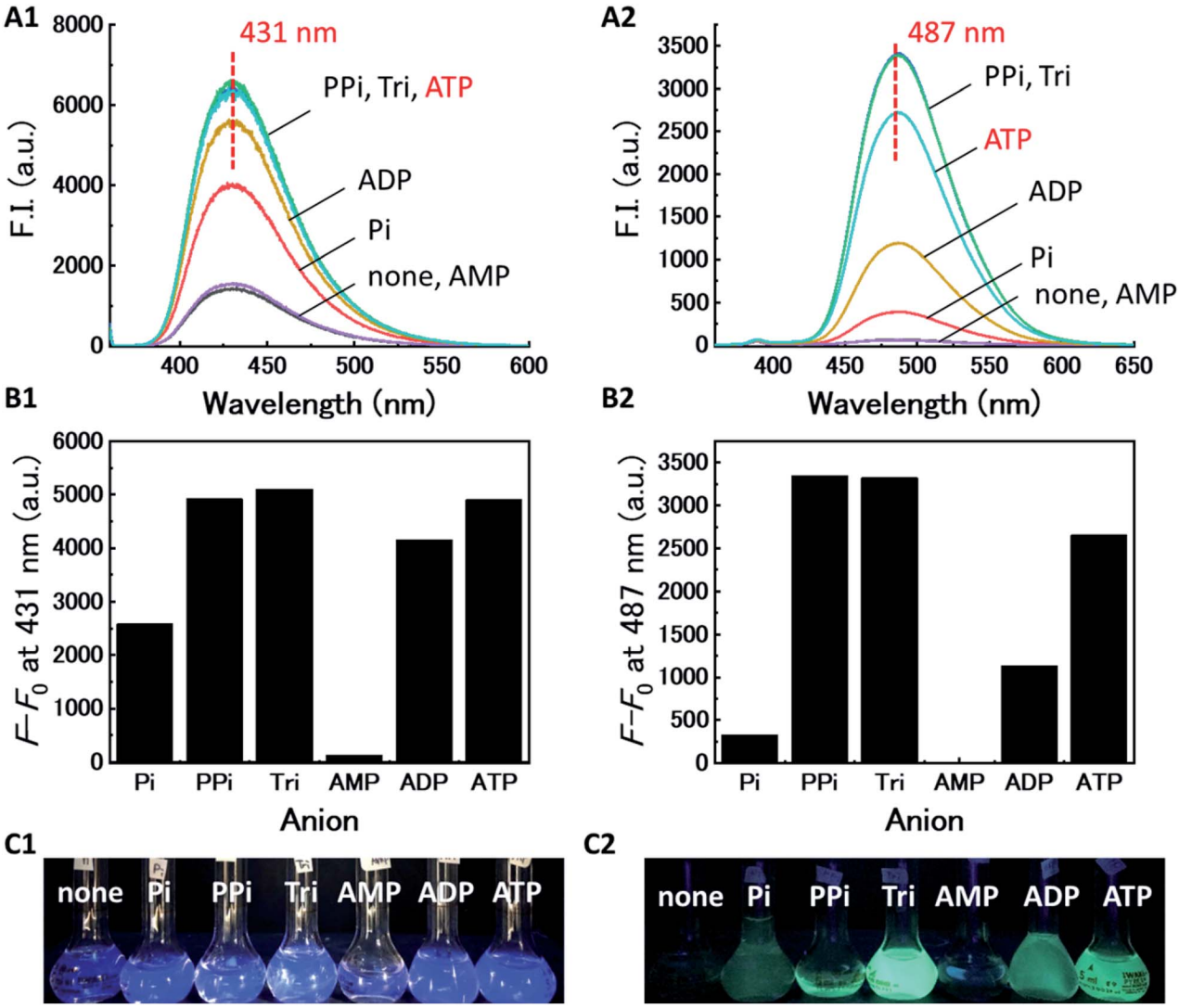

Fig. 2 (A) Fluorescence spectra of **Cu-dpa-QZ1** for (A1) and **Cu-dpa-QZ2** for (A2) with phosphoric acid derivatives (Pi, PPi, Tri, AMP, ADP, and ATP) in 1% DMSO – 99% water (v/v), pH 7.4 adjusted by HEPES/NaOH buffer, at 25 °C ($\lambda_{ex}^{dpa\text{-}QZ1}$ = 355 nm, $\lambda_{ex}^{dpa\text{-}QZ2}$ = 345 nm). (B) $F–F_0$ is the fluorescence intensity difference at fluorescence maximum wavelength of **Cu-dpa-QZ1** for (B2) and **Cu-dpa-QZ2** for (B2). [probe] = 10 μM, [$Cu(NO_3)_2$] = 20 μM, [phosphoric acid] = 1.0 mM, [HEPES buffer] = 5.0 mM. (C) UV irradiation images of **Cu-dpa-QZ1** for (C1) and **Cu-dpa-QZ2** for (C2) with phosphoric acid derivatives.

Results and discussion

First, the effect of acidity on the fluorescence of **dpa-QZ1** and **dpa-QZ2** were investigated, and both these probes exhibited weak fluorescence under acidic condition. The fluorescence intensities increased gradually with the continuous addition of the sodium hydroxide solution and reached a maximum around pH 7 (Fig. S1, ESI†). These observations can be attributed to the protonation of the nitrogen atoms of the dpa unit under acidic conditions, which cause the photo-induced electron transfer (PET) from the quinazoline fluorophore to the dpa moiety, leading to fluorescence quenching. As the pH increased, the nitrogen atom of the dpa unit underwent deprotonation, which resulted in the fluorescence recovery by PET suppression.

Next, the responses of the probes to the presence of various metals were investigated by the addition of the metal ion—Cu^{2+}, Co^{2+}, Ni^{2+}, Zn^{2+}, Pb^{2+}, and Cd^{2+} containing salts [metal $(NO_3)_2$] into the aqueous solutions of **dpa-QZ1** and **dpa-QZ2** at pH 7.4. Remarkably, the fluorescence of **dpa-QZ1** and **dpa-QZ2** was quenched by the addition of Ni^{2+} and Cu^{2+}. Particularly, the fluorescence intensity decreased significantly with the addition of Cu^{2+} (Fig. 1). These results indicate that the fluorescence is quenched in the presence of the Ni^{2+} or Cu^{2+} ions due to the ligand-to-metal charge transfer (LMCT) from the excited state of the quinazoline ligands to metal ions. The difference between the fluorescence response to Ni^{2+} and Cu^{2+} could be attributed to the difference of the binding affinities of dpa to each metal ion due to difference in the ion size.

Table 1 Summary of the binding constants (K_{app}, M^{-1}) of **Cu-dpa-QZ1** and **Cu-dpa-QZ2** to various phosphoric acid derivatives[a]

Phosphoric acid derivatives	K_{app} [M^{-1}]	
	Cu-dpa-QZ1	**Cu-dpa-QZ2**
Pi	8.4×10^3	1.2×10^3
PPi	2.2×10^5	7.3×10^4
Tri	5.4×10^5	7.2×10^4
AMP	n.d.[b]	n.d.[b]
ADP	1.5×10^4	4.7×10^3
ATP	7.3×10^4	3.8×10^4

[a] Fluorescence measurement for phosphoric acid titration curves were performed in 1% DMSO – 99% water (v/v), pH 7.4 adjusted by HEPES/NaOH buffer, at 25 °C ($\lambda_{ex}^{dpa\text{-}QZ1}$ = 355 nm, $\lambda_{ex}^{dpa\text{-}QZ2}$ = 345 nm). [probe] = 10 μM, [$Cu(NO_3)_2$] = 20 μM, [phosphoric acids] = 0–4.0 mM, [$NaNO_3$] = 0.10 M, [HEPES buffer] = 5.0 mM. [b] n.d. = Not determined due to insufficient fluorescence enhancement even in the presence of 1.5 mM AMP.

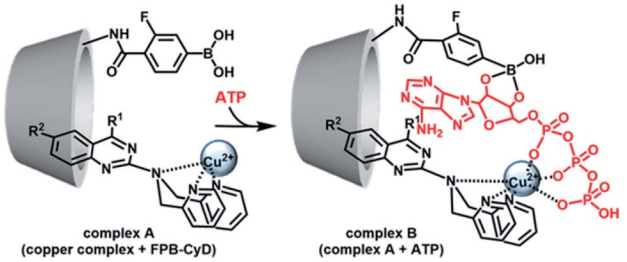

Fig. 3 Proposed scheme for ATP-detection by the multipoint recognition system using copper complex and **FPB-CyD**.

The binding constants of the quinozaline probes to Cu^{2+} were calculated by the curve fitting method (5.7×10^5 M^{-1} for **dpa-QZ1** and 1.1×10^7 M^{-1} for **dpaQZ2**; Fig. S2, ESI†), and indicated the formation of complexes in a 1 : 1 ratio with the copper ions. Because **dpa-QZ2** has electron donating groups attaching to the quinazoline framework, methoxy group at the position 4 and di-methylamino group at the position 6, the binding capability of **dpa-QZ2** to Cu^{2+} is higher than that of **dpa-QZ1**. The difference of the fluorescence response to Ni^{2+} between these two probes is also due to the difference of the electron density of dpa group. These results prompted us to investigate the use of these dpa–copper complexes (**Cu-dpa-QZ1** and **Cu-dpa-QZ2**) for sensing phosphate anions.

We evaluated the recognition abilities of these two metal complexes in the presence of 100 equivalents of phosphate under investigation, and monophosphate (Pi), pyrophosphate (PPi), triphosphate (Tri), AMP, ADP, and ATP were assayed under these conditions. The fluorescence of **Cu-dpa-QZ1** dramatically recovered upon addition of each of the phosphates, except AMP (Fig. 2). The fluorescence of **Cu-dpa-QZ2** was fully recovered by the addition of PPi, Tri, and ATP, whereas, it recovered by half upon ADP addition. These results clearly indicate that the interactions between the copper ion and the phosphoric acid derivatives weakened the coordination of the dpa moieties to Cu^{2+}, which caused the fluorescence

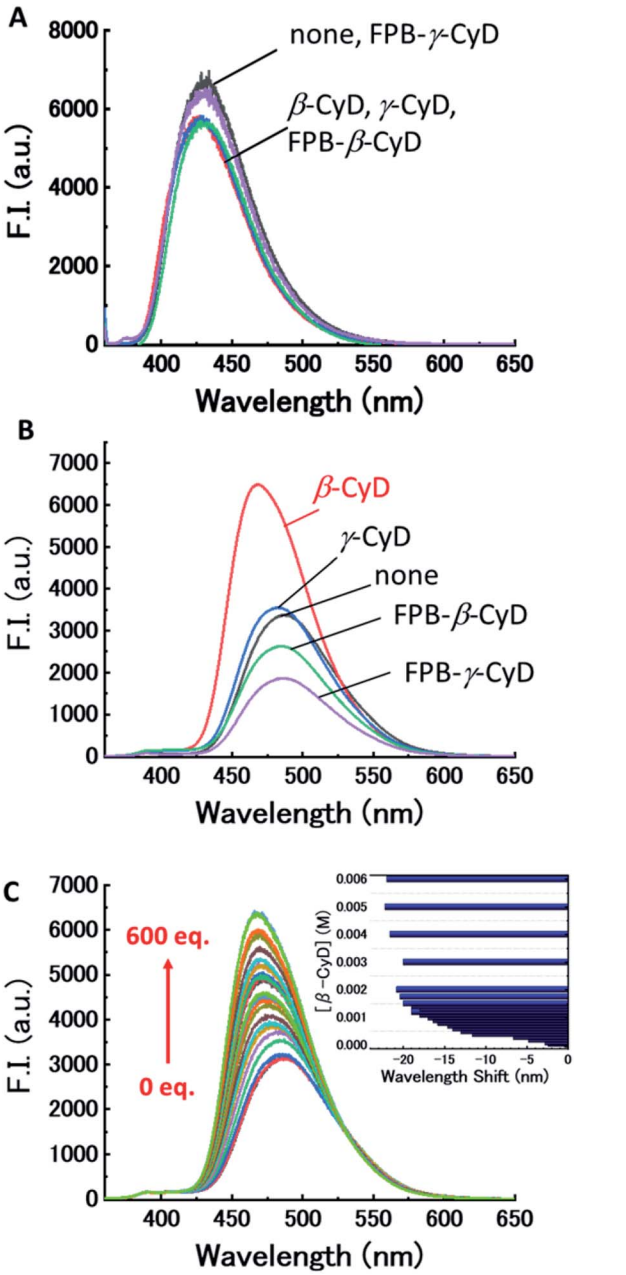

Fig. 4 Fluorescence-response of (A) **dpa-QZ1** and (B) **dpa-QZ2** to CyDs and modified-CyDs with FPB in 1% DMSO – 99% water (v/v), pH 7.4 adjusted by HEPES/NaOH buffer, at 25 °C ($\lambda_{ex}^{dpa\text{-}QZ1}$ = 355 nm, $\lambda_{ex}^{dpa\text{-}QZ2}$ = 345 nm). [probe] = 10 μM, [CyD] = 5.0 mM, [**FPB-CyD**] = 0.50 mM, [$NaNO_3$] = 0.10 M, [HEPES buffer] = 5.0 mM. Notably, for CyDs the concentration that exhibited the highest fluorescence response to the probe was adopted, whereas for **FPB-CyDs** the approximate saturation concentration was used. (C) Fluorescence-response of **dpa-QZ2** to β-CyD (0–6.0 mM) in 1% DMSO – 99% water (v/v), and their wavelength shifts, pH 7.4 adjusted by HEPES/NaOH buffer, at 25 °C (λ_{ex} = 345 nm). [**dpa-QZ2**] = 10 μM, [HEPES buffer] = 5.0 mM, [$NaNO_3$] = 0.10 M.

recovery by the inhibition of LMCT from the excited quinazoline core to Cu^{2+}. The binding constants (K_{app}, M^{-1}) of the copper complexes, obtained from the titration curves (Fig. S3 and S4, ESI†), indicated weak binding to AMP, moderate binding to Pi

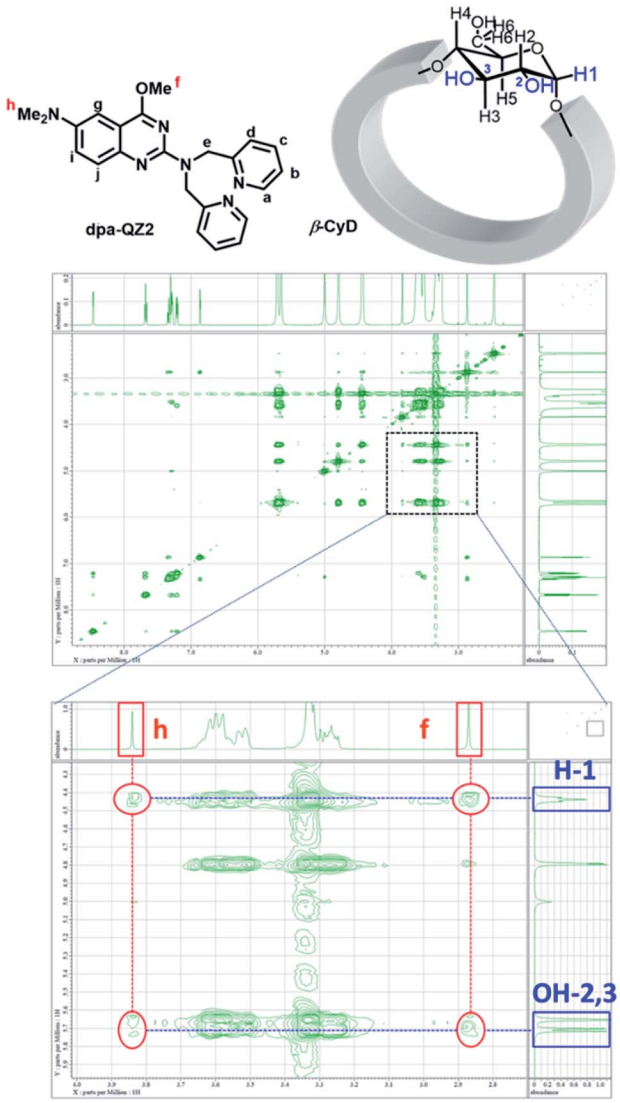

Fig. 5 The NMR assignments and NOESY spectra of **dpa-QZ2**/β-CyD in 100% d_6-DMSO.[30] [**dpa-QZ2**] = 8 mM, [β-CyD] = 16 mM.

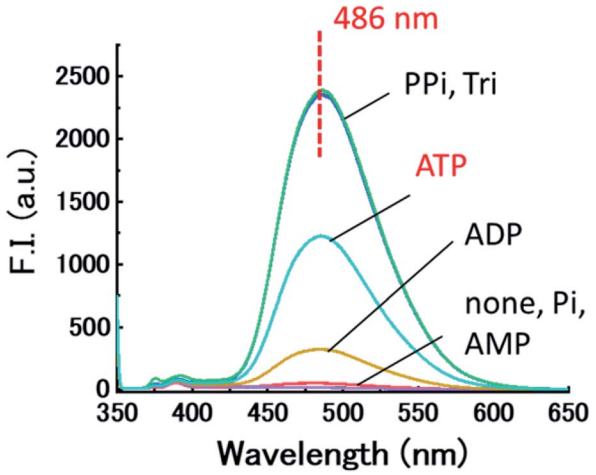

Fig. 6 Fluorescence spectra of **Cu-dpa-QZ2** with phosphoric acid derivatives (Pi, PPi, Tri, AMP, ADP and ATP) in the presence of **FPB-γ-CyD** in 1% DMSO – 99% water (v/v), pH 7.4 adjusted by HEPES/NaOH buffer, at 25 °C. $F–F_0$ is the fluorescence intensity difference at fluorescence maximum wavelength (λ_{ex} = 345 nm). [**dpa-QZ2**] = 10 μM, [$Cu(NO_3)_2$] = 20 μM, [**FPB-γ-CyD**] = 0.50 mM, [phosphoric acid] = 1.0 mM, [HEPES buffer] = 5.0 mM.

and ADP, and very strong binding to PPi, Tri, and ATP (Table 1). The binding constant of **Cu-dpa-QZ1** to ATP (7.3×10^4 M^{-3}) was comparable to that of **Cu-dpa-QZ2** (1.2×10^4 M^{-3}), whereas **Cu-dpa-QZ1** exhibited a substantially higher binding constant to ADP (1.5×10^4 M^{-3}) than **Cu-dpa-QZ2** (4.7×10^3 M^{-3}), indicating that **dpa-QZ2** has higher ATP selectivity than **dpa-QZ1**.

Having determined the binding abilities and the fluorescence behaviour of the developed probes, we turned to examine the use of cyclodextrins (CyDs) to improve the selectivity and sensitivity of the ATP sensing, based on a reported multipoint recognition system.[28,29] It was assumed that the introduction of the dpa probe into the hydrophobic cavity of 3-fluorophenyl boronic acid (FPB)-modified CyD could likely allow the binding of ATP, wherein, the Cu–dpa recognizes the phosphoric acid unit of ATP, and the FPB recognizes the 1,2-*cis*-diol unit of the adenosine simultaneously (Fig. 3).

First, the fluorescence responses of **dpa-QZ1** and **dpa-QZ2** to β-CyD, γ-CyD, **FPB-β-CyD**, and **FPB-γ-CyD** were evaluated. Despite the lack of particular differences in the responses of **dpa-QZ1** to the CyDs, the fluorescence intensity of **dpa-QZ2** was enhanced in the presence of β-CyD, indicating the interaction of **dpa-QZ2** with the hydrophobic cavity of β-CyD (Fig. 4A and B). Notably, the NOESY spectrum of the mixture of **dpa-QZ2** and β-CyD exhibited interactions between the protons of the quinazoline and those of the CyD's concave side (Fig. 5), thus confirming the interaction of the probe with the CyD. Furthermore, the fluorescence intensity increased upon mixing **dpa-QZ2** and β-CyD, and a blue shift in the fluorescence was observed in the presence of DMSO in a concentration-dependent manner (Fig. 4C and S5, ESI†). These observations support the incorporation of **dpa-QZ2** into the cavity of the CyD and the stabilization by hydrophobic interactions.

The fluorescence responses of **dpa-QZ1** and **dpa-QZ2** to the metal ions in the presence of CyDs and the FPB-modified CyDs exhibited the same levels of responses as those in the absence of CyDs (Fig. S6 and S7 ESI†). The fluorescence recovery ratios (F/F_0) calculated from the emission intensities of copper complexes with CyDs and the phosphoric acid derivatives were used to evaluate the selectivity and the sensitivity of the ATP sensing, where F is the relative fluorescence intensity (after the addition of phosphoric acids), and F_0 is that of initial state (before the addition of phosphoric acids) (Fig. 6 and Table 2). In the case of **Cu-dpa-QZ1**, the presence of CyDs did not affect the fluorescence recovery ratios and sensitivities (Table 2 and Fig. S8, ESI†). In contrast, the sensitivities to PPi, Tri and ATP were increased by using **Cu-dpa-QZ2** in the presence of **FPB-γ-CyD** (PPi: F/F_0 from 55 to 133, Tri: F/F_0 from 55 to 135, ATP: F/F_0 from 44 to 69) and those to Pi, AMP, and ADP were not affected by the presence of **FPB-γ-CyD** (Pi: F/F_0 6.2 and 2.9, AMP: F/F_0 <1 and < 1, ADP: F/F_0 19 and 18) (Table 2, Fig. 6 and S9, ESI†). However, the limit of detections (3 × standard deviation of the regression line/slope), calculated from the values of ($F–F_0$) and

Table 2 Summary of the fluorescence recovery ratio (F/F_0) of **Cu-dpa-QZ1** and **Cu-dpa-QZ2** in the presence of **FPB-γ-CyD** with various phosphoric acid derivatives against the initial state at fluorescence maximum wavelength[a]

Phosphoric acid derivatives	Fluorescence recovery ratio (F/F_0)[b]									
	Cu-dpa-QZ1					**Cu-dpa-QZ2**				
	None	β-CyD	γ-CyD	**FPB-β-CyD**	**FPB-γ-CyD**	None	β-CyD	γ-CyD	**FPB-β-CyD**	**FPB-γ-CyD**
Pi	2.8	2.5	1.9	3.1	2.4	6.2	2.5	2.1	4.3	2.9
PPi	4.5	3.9	2.6	8.7	5.5	55	14	14	65	133
Tri	4.6	3.9	2.7	8.6	5.3	55	14	14	64	135
AMP	1	1.2	<1	1.5	1.3	<1	<1	<1	<1	<1
ADP	4.0	3.6	2.5	6.6	4.5	19	8.3	6.2	16	18
ATP	4.5	3.7	2.6	8.1	5.2	44	12	12	47	69

[a] Fluorescence measurements for the selectivity of phosphoric acid derivatives were performed in 1% DMSO – 99% water (v/v), pH 7.4 adjusted by HEPES/NaOH buffer, at 25 °C ($\lambda_{ex}^{dpa\text{-}QZ1} = 355$ nm, $\lambda_{ex}^{dpa\text{-}QZ2} = 345$ nm). [probe] = 10 μM, [$Cu(NO_3)_2$] = 20 μM, [phosphoric acids] = 1.0 mM, [$NaNO_3$] = 0.10 M, [HEPES buffer] = 5.0 mM. [b] Unless otherwise noted, F/F_0 indicates the relative fluorescence intensity (F) at 431 nm of **Cu-dpa-QZ1** and 486 nm of **Cu-dpa-QZ2** in the presence of 1.0 mM of the phosphoric acid derivatives against that of the initial state (F_0).

the concentrations of ATP (Fig. S4F and S10, ESI†) did not exhibit any significant difference. They were found to be 1.50 and 0.32 μM in the presence and absence of **FPB-γ-CyD**, respectively. Further investigation using modified recognition systems with structurally-tuned quinazoline fluorophores and boronic acid-tethered CyDs is expected to further confirm the role of the boronic acid moiety.

Conclusions

In conclusion, novel quinazoline fluorescent probes, **dpa-QZ1**, and **dpa-QZ2** were developed, which enabled the recognition of various phosphoric acid derivatives by fluorescence enhancement. While both probes showed similar levels of response to metal ions, their levels of response to phosphoric acid derivatives and CyDs were different. The ATP selectivity of **dpa-QZ2** was better than that of **dpa-QZ1**, and in the presence of β-CyD, **dpa-QZ2** showed fluorescence enhancement, indicating the binding of **dpa-QZ2** to the hydrophobic cavity of β-CyD. The recognition system comprising **dpa-QZ2** and FPB-modified γ-CyD demonstrated higher sensitivity to ATP ($F/F_0 = 69$). Overall, 2-amioquinazolines display high fluorescence intensities and can serve as efficient probes or sensors for enabling sensitive, versatile, and wide-ranging applications, such as real-time monitoring of the intracellular ATP concentration, which facilitates to the elucidation of vital biological phenomena. Furthermore, ATP detection with higher sensitivity and selectivity can be achieved through structural modification of the quinazoline fluorophore and CyDs.

Conflicts of interest

There are no conflicts to declare.

Acknowledgements

This work was supported by a Grant-in-Aid for Scientific Research (C) (18K06587) from the Japan Society for the Promotion of Science and MEXT, Japan.

Notes and references

1 F. Ozogul, T. Kda, P. C. Quantick and Y. Ozogul, *Int. J. Food Sci. Technol.*, 2000, **35**, 549.
2 Y. Lian, H. Jiang, J. Feng, X. Wang, X. Hou and P. Deng, *talanta*, 2016, **150**, 485.
3 B. Liu, M. Ozaki, H. Hisamoto, Q. Luo, Y. Utsumi, T. Hattori and S. Terabe, *Anal. Chem.*, 2005, **77**, 573.
4 Y. Wu, J. Wen, H. Li, S. Sun and Y. Xu, *Chin. Chem. Lett.*, 2017, **28**, 1916.
5 A. Ojida, I. Takashima, T. Kohira, H. Nonaka and I. Hamachi, *J. Am. Chem. Soc.*, 2008, **130**, 12095.
6 L. Xiao, S. Sun, Z. Pei, Y. Pei, Y. Pang and Y. Xu, *Biosens. Bioelectron.*, 2015, **65**, 166.
7 H. Imamura, K. P. Huynh Nhat, H. Togawa, K. Saito, R. Iino, Y. Kato-Yamada, T. Nagai and H. Noji, *Proc. Natl. Acad. Sci. U. S. A.*, 2009, **106**, 15651.
8 F. Li, X. Hu, F. Wang, B. Zheng, J. Du and D. Xiao, *Talanta*, 2018, **179**, 285.
9 T. Hu, W. Na, X. Yan and X. Su, *Talanta*, 2017, **165**, 194.
10 Y. Tsuchido, A. Yamasawa, T. Hashimoto and T. Hayashita, *Anal. Sci.*, 2018, **34**, 1125.
11 L. G. Pathberiya, N. Barlowa, T. Nguyen, B. Graham and K. L. Tuck, *Tetrahedron*, 2012, **68**, 9435.
12 B. A. Wong, S. Friedle and S. J. Lippard, *Inorg. Chem.*, 2009, **48**, 7009.
13 A. Ojida, Y. Mito-oka, M. Inoue and I. Hamachi, *J. Am. Chem. Soc.*, 2002, **124**, 6256.
14 A. Ojida, Y. Mito-oka, K. Sada and I. Hamachi, *J. Am. Chem. Soc.*, 2004, **126**, 2454.
15 A. Ojida, Y. Miyahara, J. Wongkongkatep, S. Tamura, K. Sada and I. Hamachi, *Chem.–Asian J.*, 2006, **1**, 555.
16 J. B. Kim, Y. M. Lee, J. Ryu, W. J. Kim, G. Keum and E. K. Bang, *Bioconjugate Chem.*, 2016, **27**, 1850.
17 G. Crini, *Chem. Rev.*, 2014, **114**, 10940.
18 A. Harada, Y. Takashima and H. Yamaguchi, *Chem. Soc. Rev.*, 2009, **38**, 875.

19 A. Antelo, A. Jover, L. Galantini, F. Meijide, M. A. Alcalde, N. V. Pavel and J. V. Tato, *J. Inclusion Phenom. Macrocyclic Chem.*, 2011, **69**, 245.
20 M. Kumai, S. Kozuka, M. Samizo, T. Hashimoto, I. Suzuki and T. Hayashita, *Anal. Sci.*, 2012, **28**, 121.
21 A. Ueno, T. Kuwabara, A. Nakamura and F. Toda, *Nature*, 1992, **356**, 136.
22 G. Wenz, *Angew. Chem., Int. Ed. Engl.*, 1994, **33**, 803.
23 D. Patra, H. Zhang, S. Sengupta and A. Sen, *ACS Nano*, 2013, **7**, 7674.
24 R. Challa, A. Ahuja, J. Ali and R. K. Khar, *AAPS PharmSciTech*, 2005, **6**, 329.
25 Y. Suzuki, J. Sawada, P. Hibner, H. Ishii, K. Matsuno, M. Sato, B. Witulski and A. Asai, *Dyes Pigm.*, 2017, **145**, 233.
26 E. A. Raux, Master's thesis, Georgia State University, 2010.
27 L. Zhu, J. Jin, C. Liu, C. Zhang, Y. Sun, Y. Guo, D. Fu, X. Chen and B. Xu, *Bioorg. Med. Chem.*, 2011, **19**, 2797.
28 Y. Tsuchido, S. Fujiwara, T. Hashimoto and T. Hayashita, *Chem. Pharm. Bull.*, 2017, **65**, 318.
29 T. Yamada, S. Fujiwara, K. Fujita, Y. Tsuchido, T. Hashimoto and T. Hayashita, *Molecules*, 2018, **23**, 635.
30 H. J. Schneider, F. Hacket, V. Rüdiger and H. Ikeda, *Chem. Rev.*, 1998, **98**, 1755.

